Lawrence Berkeley National Laboratory
LBL Publications

Title

Extreme ultraviolet induced chemistry in polymer thin films

Permalink

https://escholarship.org/uc/item/8471t341

Journal

Proceedings of SPIE--the International Society for Optical Engineering, 13428

ISSN

0277-786X

Authors

Kostko, Oleg

Im, Honggu

Luttgenau, Bernhard

et al.

Publication Date

2025-04-22

DOI

10.1117/12.3051486

eScholarship.org Powered by the California Digital Library
University of California

Extreme ultraviolet induced chemistry in polymer thin films

Oleg Kostko,[1*] Honggu Im,[1] Bernhard Luttgenau,[1] Alex Aguilar Oliveros,[2] Cuc Ngan Tran,[2] Dahyun Oh[2]
[1]Center for X-Ray Optics, Lawrence Berkeley National Laboratory, Berkeley, CA, USA
[2]San Jose State University, San Jose, CA, USA

ABSTRACT

Extreme ultraviolet (EUV) lithography relies on the development of advanced photoresist materials with optimized sensitivity, resolution, and etch resistance. Understanding the fundamental mechanisms of EUV-induced chemical transformations is crucial for improving resist performance. In this study, we investigate the EUV-induced degradation of poly(tert-butyl methacrylate) (PtBMA) and its copolymer with poly(4-hydroxystyrene) (P(tBMA-co-HS)). Using mass spectrometry, film thickness measurements, and Fourier-transform infrared (FTIR) spectroscopy, we analyze outgassing behavior, material loss, and molecular transformations in these polymers. Our results reveal that PtBMA undergoes significant fragmentation beyond simple deprotection, leading to higher outgassing and film shrinkage, while P(tBMA-co-HS) exhibits enhanced stability. These findings provide insights into polymer composition effects on EUV resist behavior and inform strategies for designing more robust photoresists for next-generation lithographic applications.

Keywords: extreme ultraviolet (EUV), extreme ultraviolet lithography, lithography, photoresist, secondary electrons, polymers, electron-induced chemistry

1. INTRODUCTION

Extreme ultraviolet (EUV) lithography has emerged as a critical technology for advanced semiconductor manufacturing, enabling patterning at the nanometer scale. However, the successful implementation of EUV lithography depends on the development of highly efficient photoresist materials that exhibit adequate sensitivity, resolution, and etch resistance. One of the primary challenges in EUV resist design is understanding the fundamental mechanisms of radiation-induced chemical transformations and material degradation, which directly impact resist performance.

In EUV lithography, photon absorption triggers the emission of a primary electron, which, through inelastic scattering, generates multiple slower secondary electrons. These secondary electrons play a crucial role in pattern formation in modern EUV photoresists. In metal-oxide (MOx) resists, both EUV photons and emitted electrons cleave organic ligands that protect metal-oxide clusters, leading to condensation and the formation of metal-oxygen bonds.[1–3] In chemically amplified resists (CAR), slow secondary electrons interact with photoacid generator (PAG) molecules, producing acids that react with polymer protecting groups, altering polymer solubility.[4,5] Additionally, polymer-based resists undergo a series of photon- and electron-induced reactions, resulting in bond scission and molecular fragmentation. These processes may lead to unwanted volatile byproduct formation and structural changes in the resist film, impacting patterning performance. A detailed understanding of these mechanisms is essential for optimizing resist formulations, improving pattern fidelity, and minimizing material loss and outgassing.

In this study, we investigate the EUV-induced chemical transformations in poly(tert-butyl methacrylate) (PtBMA) and its copolymer with poly(4-hydroxystyrene) (P(tBMA-co-HS)). PtBMA has been widely used as a model polymer for EUV CAR studies due to its well-defined acid-catalyzed deprotection chemistry, which involves the cleavage of tert-butyl groups and the release of isobutylene. We employ a combination of mass spectrometry, film thickness measurements, and Fourier-transform infrared (FTIR) spectroscopy to characterize the chemical and physical changes occurring in these materials during EUV irradiation. Mass spectrometry allows for the identification of volatile species released upon exposure, providing insights into outgassing behavior. Film thickness measurements reveal the extent of material loss, while FTIR spectroscopy enables the analysis of molecular transformations within the polymer matrix. By comparing the EUV response of PtBMA and P(tBMA-co-HS), we aim to elucidate the role of polymer composition in resist degradation and identify pathways to enhance resist performance. The findings from this study contribute to the ongoing efforts in designing next-generation EUV resists with improved chemical stability and patterning capabilities.

* E-mail: okostko@lbl.gov

Advances in Patterning Materials and Processes XLII, edited by Ryan Callahan, Anuja De Silva, Proc. of SPIE Vol. 13428, 134282K · © 2025 SPIE
0277-786X · doi: 10.1117/12.3051486

2. EXPERIMENTAL SECTION

In this study, PtBMA and a 6:4 random copolymer of tert-butyl methacrylate and 4-hydroxystyrene (P(tBMA-co-HS)) were used as photoresist polymer matrices (Fig. 1). Thin films (~15 nm) of these materials were spin-coated onto silicon wafers. Double-side-polished wafers were used for most experiments, while single-side-polished wafers were used for outgassing measurements.

EUV exposures were conducted at beamline 12.0.1.2 of the Advanced Light Source, Lawrence Berkeley National Laboratory. The wafers were scanned in front of a 5 mm × 1 mm EUV spot, with scanning velocity determining the effective EUV dose. Samples were exposed to doses ranging from 25 to 300 mJ/cm^2. Film thickness before and after exposure was measured using a Woollam M-2000 spectroscopic ellipsometer.

FTIR measurements were performed using a Thermo Nicolet 6700 spectrometer. To obtain a background signal, part of the polymer film was removed with acetone, exposing the bare Si wafer. Before data collection, samples were purged with N_2 gas to eliminate gaseous CO_2 and water contamination.

Outgassing measurements during EUV exposure followed a recently developed approach.[6] Briefly, samples were continuously exposed to EUV radiation while a residual gas analyzer (RGA) collected mass spectra every 3.5 seconds, identifying species released from the polymer as EUV dose increased.

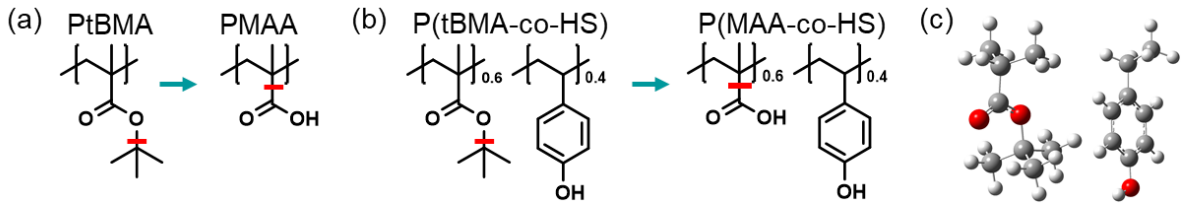

Figure 1. Monomer structures of (a) PtBMA and (b) P(tBMA-co-HS), highlighting possible bond cleavage sites in red and conversion to poly(methacrylic acid) (PMAA) or copolymer of methacrylic acid and 4-hydroxystyrene (P(MAA-co-HS)). (c) Monomer units of tBMA and 4-hydroxystyrene used in DFT calculations.

To assist in assigning peaks in the FTIR spectra, density functional theory (DFT) calculations were performed. Monomer units (4-hydroxystyrene, tert-butyl methacrylate, and methacrylic acid) were optimized using the Gaussian 9 computational package[7] with the ωB97X-D functional and a 6-311++G(d,p) basis set. The polymer matrix was modeled using the polarizable continuum model (PCM). Vibrational spectra were obtained through frequency calculations of the optimized structures.

3. RESULTS AND DISCUSSION

3.1 Outgassing

Figure 2a,b presents mass spectra of molecules outgassed during EUV exposure of static polymer samples. These spectra were collected using a previously described approach.[6] To establish a baseline, background outgassing was measured for the first 60 seconds with the EUV light blocked by a shutter. Once the shutter was opened, the sample was exposed to EUV radiation, initiating photon- and electron-induced chemical reactions that led to the release of small molecules.

The most prominent peaks in the mass spectra correspond to the outgassing of isobutylene (characterized by intense signals at m/z 27, 28, 39, 41, and 56) and CO_2 (m/z 12, 16, 28, and 44). This identification is further supported by the model mass spectrum shown in Figure 2c, which was generated using data from the National Institute of Standards and Technology (NIST) database.[8] While some peaks near m/z 70, as well as the high yield of H_2, remain unassigned using a combination of isobutylene and CO_2, the majority of the observed outgassing can be attributed to these two species.

Figure 3 illustrates the time-dependent outgassing signals for PtBMA and P(tBMA-co-HS) films. Since EUV exposure time correlates with total EUV dose, the time axis can be converted into EUV dose, with a conversion factor of 1.25 mJ/cm^2/s used in this study. The PtBMA sample exhibits a rapid increase in outgassing upon EUV exposure, reaching a maximum around 75 seconds, followed by a pressure decline. In contrast, the P(tBMA-co-HS) sample shows a similar saturation time but experiences a slower decay in outgassing signal.

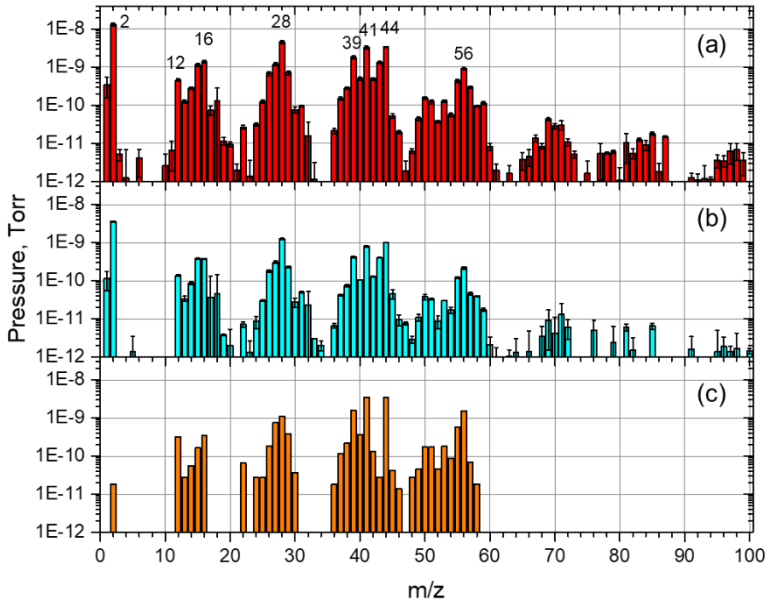

Figure 2. Mass spectra of outgassed species collected during EUV exposure of (a) PtBMA and (b) P(tBMA-co-HS). (c) A reference mass spectrum generated using data from the NIST database, representing an equal ratio of isobutylene (1-propene, 2-methyl-) and CO_2. The intensity of this spectrum is scaled to match that of PtBMA.

Notably, the peak outgassing pressure for PtBMA is approximately four times higher than that for P(tBMA-co-HS), despite the fact that the concentration of tBMA monomers differs by only a factor of ~1.4 (considering film thicknesses of 18 nm for P(tBMA-co-HS) and 17 nm for PtBMA). The observed decay in PtBMA's outgassing signal following its initial peak may be attributed to the gradual depletion of volatile species within the film. The mass spectra shown in Figures 2a and 2b were obtained by averaging the first 20 seconds of the time-dependent outgassing signal for individual mass channels.

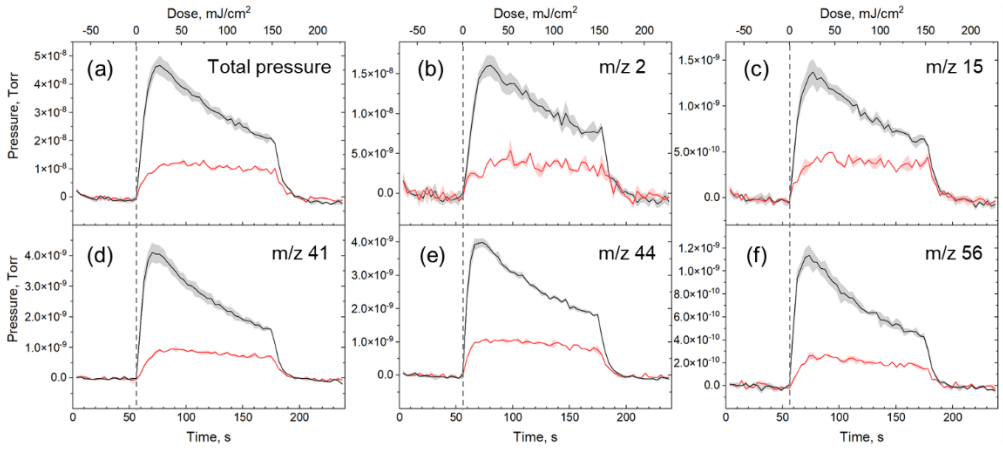

Figure 3. Dose dependent outgassing signal for (a) total ion signal, (b) m/z 2, (c) m/z 15, (d) m/z 41, (e) m/z 44, and (f) m/z 56, measured for PtBMA (black line) and P(tBMA-co-HS) (red line).

3.2 Thickness loss

The normalized film thickness of EUV-exposed polymer samples is shown in Figure 4a using symbols and dashed lines. As the EUV dose increases, film thickness decreases accordingly. Notably, PtBMA films experience significantly greater thickness loss compared to P(tBMA-co-HS) films. Assuming that thickness loss primarily results from EUV-induced deprotection—where tert-butyl groups are cleaved and isobutylene is released—the final film thickness can be estimated

for fully deprotected polymers, as previously discussed.[9] In this model, deprotection of the t-butyl methacrylate unit is assumed to yield methacrylic acid and the next decarboxylation step will lead to CO_2 emission and conversion to propylene.

As shown in Table 1, complete deprotection would reduce the thickness of PtBMA to 61% of its original value, while P(tBMA-co-HS) would retain 75% of its initial thickness. From Figure 4a, PtBMA exposed to 300 mJ/cm^2 shrinks to 59% of its original thickness, exceeding the expected loss from deprotection alone. Additional decarboxylation (observed previously[10,11] and also shown in Figure 3e), leading to a film thickness reduction to 34% of its initial value, which is significantly lower than the thickness remaining after exposure to 300 mJ/cm^2. This suggests that CO_2 emission and additional mechanisms, such as complex molecular fragmentation,[12] could lead to densification and further thickness reduction. For P(tBMA-co-HS), exposure to 300 mJ/cm^2 results in a thickness loss of 10% of its original value, what is above the theoretical loss due to complete polymer deprotection (25%).

Table 1. Molar masses, densities, and final thickness ratios for PtBMA, PHS, P(tBMA-co-HS), poly(methacrylic acid) (PMAA), P(MAA-co-HS), and polypropylene (PP). Densities and molar masses of P(tBMA-co-HS) and P(MAA-co-HS) were calculated as weighted averages of those for PHS and PtBMA (or PMAA), based on their respective abundances in the copolymers. Two final thickness ratios are presented: one based on the emission of isobutylene and conversion to PMAA, and the other assumes polymer decarboxylation and conversion to PP.

	PtBMA	PHS	P(tBMA-co-HS)	PMAA	P(MAA-co-HS)	PP
ρ (g/cm3)	1.022	1.160	1.077	1.015	1.073	0.900
M (g/mol)	142.20	120.15	133.38	86.09	99.71	42.08
Final thickness ratio, PMAA	0.61	–	0.75	–	–	–
Final thickness ratio, PP	0.34	–	0.59	–	–	–

It is useful to compare polymer behavior within the typical EUV dose range for resist applications (25–50 mJ/cm^2). In this range, P(tBMA-co-HS) exhibits minimal thickness loss (0.4–1.2%), whereas PtBMA loses 4.4–9.4% of its thickness. This suggests that direct photon- and electron-induced deprotection of PtBMA is significant even at low EUV doses. Polymers with high EUV sensitivity may therefore be unsuitable for chemically amplified resists, where deprotection primarily occurs via acid-catalyzed reactions.

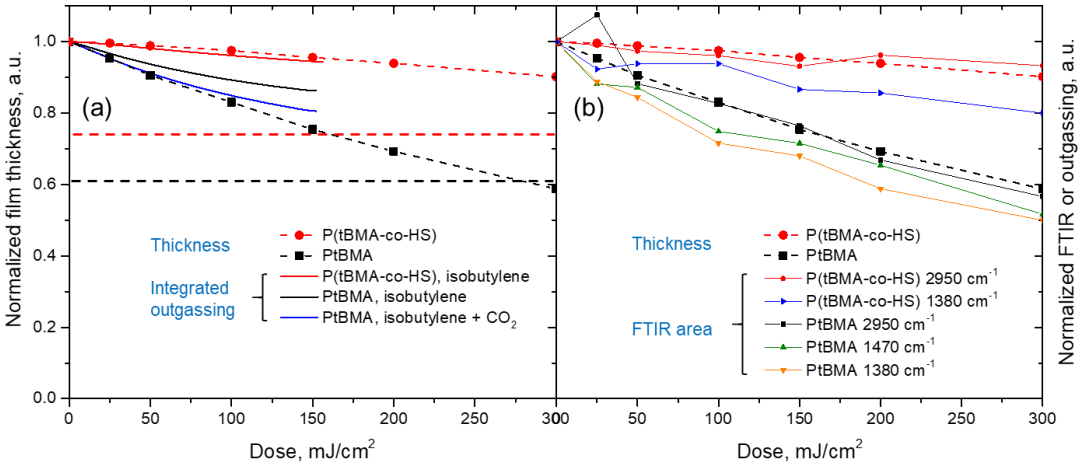

Figure 4. (a) Dose-dependent normalized film thickness for PtBMA and P(tBMA-co-HS) thin films. Horizontal dashed lines indicate the expected final film thickness for fully deprotected polymers. The normalized integrated outgassing signal, corresponding to isobutylene and CO_2 release, is compared to the thickness loss. (b) Dose-dependent normalized film thickness for PtBMA and P(tBMA-co-HS), compared to normalized FTIR peak areas.

Since the outgassing observed in Figure 3 occurs continuously during EUV exposure, the total number of outgassed molecules should correlate with the thickness loss discussed above. To quantify the total amount of outgassed molecules, we integrated the signal corresponding to the isobutylene fragment at m/z 41 (Fig. 3d). The total isobutylene amount was

then estimated by scaling the m/z 41 intensity by a factor of 3.275, derived from NIST database data to account for isobutylene fragmentation.

To compare this integrated signal with the normalized thickness loss shown in Figure 4a, a pressure normalization factor was determined. This was done by estimating the total number of available tert-butyl groups in the exposed film regions. By considering the pumping speed of the RGA system, we determined the pressure increase corresponding to the complete outgassing of isobutylene from the films. These pressure values were used as normalization factors for the integrated isobutylene outgassing pressure.

The resulting normalized pressure loss due to isobutylene outgassing is compared to the normalized film thickness loss in Figure 4a. For P(tBMA-co-HS), a strong correlation is observed, suggesting that most of the thickness loss can be attributed to isobutylene outgassing. In contrast, PtBMA exhibits a significant discrepancy between integrated isobutylene outgassing and thickness loss, indicating more extensive polymer degradation. When CO_2 emission from PtBMA is also considered, the correlation between integrated outgassing and thickness loss improves (Figure 4a). However, this improved correlation is puzzling, as the mass spectra of outgassed molecules (Figure 2) show that both polymers emit similar ratios of isobutylene and CO_2. A possible explanation is that PtBMA undergoes greater fragmentation, leading to the outgassing of larger molecular species, as seen in the mass spectrum (Figure 2a). These larger fragments may originate from main-chain scission and subsequent decomposition.

3.3 FTIR

FTIR spectra were collected from EUV-exposed regions of polymer films deposited on double-side-polished Si wafers, with selected spectra shown in Figure 5. It is immediately apparent that EUV exposure leads to a decrease in the intensity of most peaks. The degree of this decrease correlates with the thickness loss and outgassing discussed above: greater intensity reduction is observed for PtBMA, while P(tBMA-co-HS) exhibits a smaller decrease.

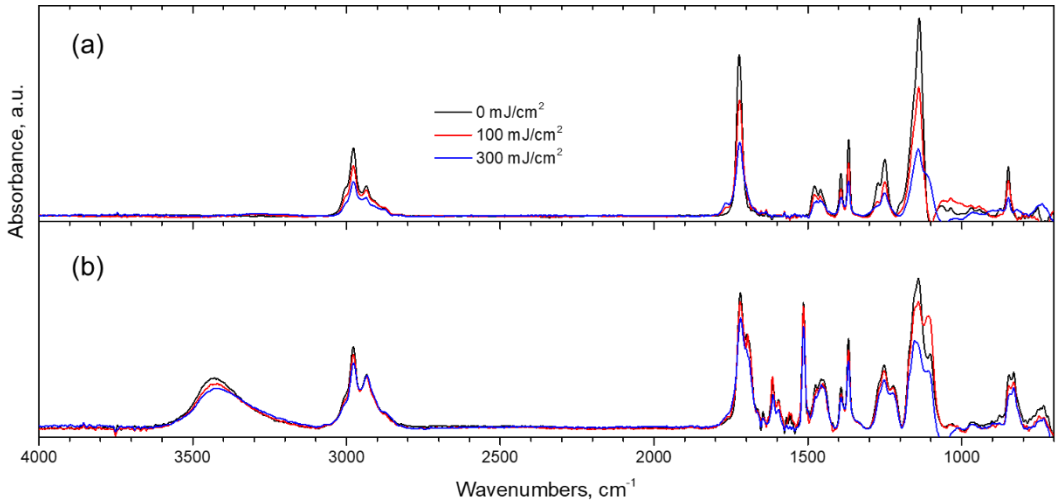

Figure 5. FTIR spectra corresponding to pristine (black line) and EUV exposed to 100 and 300 mJ/cm^2 (red and blue lines, correspondingly) films of (a) PtBMA and (b) P(tBMA-co-HS).

For analysis and peak assignment, experimental FTIR spectra were compared with spectra obtained from DFT calculations. The wavenumber axes of the calculated IR spectra were scaled by a factor of 1.07 and blue-shifted by 40 cm^{-1} to achieve the best correlation with the experimental data. For P(tBMA-co-HS), theoretical FTIR spectra were generated as a weighted combination of PtBMA and PHS spectra, based on their relative abundance in the copolymer. While this theoretical approach is useful for peak assignment, it approximates the polymer as its monomer units (Fig. 1c), which may introduce slight inaccuracies, particularly in representing the polymer backbone. Additionally, PMAA was used as a reference to illustrate vibrational spectral changes following PtBMA deprotection.

The primary features observed in the FTIR spectra include the C=O stretch (~1700 cm^{-1}), C-H stretch (~2950 cm^{-1}), O-H stretch (a broad feature around 3400 cm^{-1}), and peaks corresponding to CH_3 bending vibrations of the tert-butyl group (1470 and 1380 cm^{-1}).

In the experimental spectra, EUV exposure leads to a decrease and broadening of the C=O stretch vibration peak. This can be attributed to CO_2 loss via outgassing and changes in vibrational frequency due to tert-butyl methacrylate deprotection following isobutylene release. DFT calculations support this interpretation: in PMAA, the C=O peak is blue-shifted by ~20 cm^{-1} relative to PtBMA. Interestingly, in PtBMA, the C=O stretch peak primarily loses intensity with only minor broadening or shifting, indicating loss of both isobutylene and CO_2. In contrast, for P(tBMA-co-HS), deprotection and CO_2 loss contribute similarly to spectral changes, further confirming that PtBMA undergoes more significant transformations under EUV irradiation.

To analyze EUV-induced chemical transformations, FTIR peak areas were extracted, normalized, and plotted in Figure 4b, where they are compared to the normalized film thickness. While most peaks decrease in intensity, the C-H stretch at 2950 cm^{-1} exhibits the best correlation with film thickness for both polymers.

For PtBMA, the peaks at 1470 cm^{-1} and 1380 cm^{-1} also correlate well with film thickness but exhibit a greater degree of signal reduction than the C-H stretch. However, in P(tBMA-co-HS), the peak at 1470 cm^{-1} overlaps with benzene vibrations, making it unsuitable for quantitative analysis. It is also important to note that changes in the 2950 cm^{-1} peak may result from both deprotection and backbone cleavage, providing insight into main-chain scission in addition to deprotection.

4. CONCLUSIONS

In this study, we investigated the EUV-induced chemical transformations and material degradation in PtBMA and P(tBMA-co-HS) polymer films using mass spectrometry, film thickness measurements, and FTIR spectroscopy. Our results reveal significant differences in the EUV response of these materials, which provide insights into their suitability for resist applications. Mass spectrometry analysis of outgassed species confirmed that isobutylene and CO_2 are the primary volatile products of EUV exposure. The total outgassing signal was found to be considerably higher for PtBMA compared to P(tBMA-co-HS), despite a relatively small difference in tBMA content between the two polymers. This suggests that additional degradation pathways, such as main-chain scission, may contribute to increased volatility in PtBMA. The time-dependent outgassing behavior further highlights the rapid depletion of volatile species in PtBMA, in contrast to the more gradual outgassing decay observed in P(tBMA-co-HS). Film thickness measurements indicate that EUV exposure leads to significant material loss in both polymers, with PtBMA exhibiting a greater degree of shrinkage. At 300 mJ/cm^2, PtBMA undergoes a thickness reduction exceeding the expected loss from complete deprotection, confirming the presence of secondary fragmentation mechanisms beyond isobutylene release. FTIR analysis further supports these findings, with spectral changes revealing key differences in the chemical transformations of the two polymers. The C=O stretch peak exhibits a greater reduction in intensity for PtBMA, which correlates with its enhanced outgassing and film thickness loss. These results highlight the importance of polymer composition in determining EUV-induced degradation pathways. The higher stability and lower outgassing of P(tBMA-co-HS) suggest that copolymerization with PHS effectively mitigates excessive material loss and fragmentation, making it a better candidate for next-generation EUV resists. Future studies will extend this approach to polymer matrices combined with photoacid generators and quenchers to differentiate between EUV- and acid-induced chemistry.

5. ACKNOWLEDGEMENTS

This work was supported as part of the Center for High Precision Patterning Science (CHiPPS), an Energy Frontier Research Center funded by the U.S. Department of Energy, Office of Science, Basic Energy Sciences. Outgassing measurements were supported by the U.S. Department of Energy, Office of Science, Accelerate Initiative Award FP00017797. This research used resources of the Advanced Light Source, a U.S. DOE Office of Science User Facility under contract no. DE-AC02-05CH11231.

REFERENCES

[1] Hinsberg, W. D. and Meyers, S., "A numeric model for the imaging mechanism of metal oxide EUV resists," Advances in Patterning Materials and Processes XXXIV **10146**, 14–24, SPIE (2017).

[2] Zhang, Y., Haitjema, J., Liu, X., Johansson, F., Lindblad, A., Castellanos, S., Ottosson, N. and Brouwer, A. M., "Photochemical conversion of tin-oxo cage compounds studied using hard x-ray photoelectron spectroscopy," JM3.1 **16**(2), 023510 (2017).

[3] Bespalov, I., Zhang, Y., Haitjema, J., Tromp, R. M., van der Molen, S. J., Brouwer, A. M., Jobst, J. and Castellanos, S., "Key Role of Very Low Energy Electrons in Tin-Based Molecular Resists for Extreme Ultraviolet Nanolithography," ACS Appl. Mater. Interfaces **12**(8), 9881–9889 (2020).

[4] Hinsberg, W. D. and Wallraff, G. M., "Lithographic Resists," [Encyclopedia of Polymer Science and Technology], John Wiley & Sons, Ltd (2012).

[5] Kozawa, T. and Tagawa, S., "Radiation Chemistry in Chemically Amplified Resists," Jpn. J. Appl. Phys. **49**(3R), 030001 (2010).

[6] Lüttgenau, B., Zhang, M., Zhang, Q., Wang, C., Ruiz, R., Connolly, M. and Kostko, O., "Time-dependent characterization of total electron yield and outgassing in model EUV resist materials," International Conference on Extreme Ultraviolet Lithography 2024 **13215**, 105–113, SPIE (2024).

[7] Frisch, M. J.; Trucks, G. W.; Schlegel, H. B.; Scuseria, G. E.; Robb, M. A.; Cheeseman, J. R.; Scalmani, G.; Barone, V.; Mennucci, B.; Petersson, G. A.; Nakatsuji, H.; Caricato, M.; Li, X.; Hratchian, H. P.; Izmaylov, A. F.; Bloino, J.; Zheng, G.; Sonnenberg, J. L.; Hada, M.; Ehara, M.; Toyota, K.; Fukuda, R.; Hasegawa, J.; Ishida, M.; Nakajima, T.; Honda, Y.; Kitao, O.; Nakai, H.; Vreven, T.; Montgomery, J. A., Jr.; Peralta, J. E.; Ogliaro, F.; Bearpark, M.; Heyd, J. J.; Brothers, E.; Kudin, K. N.; Staroverov, V. N.; Kobayashi, R.; Normand, J.; Raghavachari, K.; Rendell, A.; Burant, J. C.; Iyengar, S. S.; Tomasi, J.; Cossi, M.; Rega, N.; Millam, J. M.; Klene, M.; Knox, J. E.; Cross, J. B.; Bakken, V.; Adamo, C.; Jaramillo, J.; Gomperts, R.; Stratmann, R. E.; Yazyev, O.; Austin, A. J.; Cammi, R.; Pomelli, C.; Ochterski, J. W.; Martin, R. L.; Morokuma, K.; Zakrzewski, V. G.; Voth, G. A.; Salvador, P.; Dannenberg, J. J.; Dapprich, S.; Daniels, A. D.; Farkas, Ö.; Foresman, J. B.; Ortiz, J. V.; Cioslowski, J.; Fox, D. J., "Gaussian 09, Revision D."

[8] Linstrom, P., "NIST Chemistry WebBook - SRD 69" (2017).

[9] Mueller, M., McAfee, T., Naulleau, P., Oh, D. and Kostko, O., "Study of electron-induced chemical transformations in polymers," JM3 **23**(4), 041403 (2024).

[10] Pollentier, I., Vesters, Y., Petersen, J. S., Vanelderen, P., Rathore, A., Simone, D. de and Vandenberghe, G., "Unraveling the role of photons and electrons upon their chemical interaction with photoresist during EUV exposure," Advances in Patterning Materials and Processes XXXV **10586**, 16–26, SPIE (2018).

[11] Pollentier, I., Petersen, J. S., Bisschop, P. D., Simone, D. D. and Vandenberghe, G., "Unraveling the EUV photoresist reactions: which, how much, and how do they relate to printing performance," Extreme Ultraviolet (EUV) Lithography X **10957**, 95–103, SPIE (2019).

[12] Fedynyshyn, T. H., Goodman, R. B., Cabral, A., Tarrio, C. and Lucatorto, T. B., "Polymer photochemistry at the EUV wavelength," Advances in Resist Materials and Processing Technology XXVII **7639**, 83–94, SPIE (2010).